

# Formation of undesired by-products in deNO<sub>x</sub> catalysis by hydrocarbons

Frank Radtke, René A. Köppel, Alfons Baiker \*

*Department of Chemical Engineering and Industrial Chemistry, Swiss Federal Institute of Technology, ETH-Zentrum, CH-8092 Zürich, Switzerland*

## Abstract

The catalytic performance of Cu/ZSM-5 and  $\gamma$ -alumina in the selective catalytic reduction of nitrogen oxides by alkenes in excess oxygen and the formation of potentially harmful by-products such as hydrogen cyanide, cyanic acid, ammonia, nitrous oxide and carbon monoxide have been studied by means of FT-IR-gas phase analysis. Over Cu/ZSM-5 the reduction activity was strongly influenced by the type of hydrocarbon, while there was no significant difference when starting from NO or NO<sub>2</sub>. In contrast, with  $\gamma$ -alumina NO<sub>2</sub> was reduced more efficiently than NO with both reductants. Water addition strongly suppressed the catalytic activity of  $\gamma$ -alumina. Regarding the formation of undesired by-products, substantial amounts of carbon monoxide were observed in all experiments, independently of the feed composition. The type of catalyst, the use of either NO or NO<sub>2</sub>, the alkene used as a reductant and water strongly influenced the formation of other by-products. With alumina ethene showed a lower tendency to form HCN as compared to propene and water addition further suppressed by-product formation. This contrasts the findings with Cu/ZSM-5, where HCN production was not significantly altered by the presence of water. On this catalyst HNCO was found additionally for dry feeds, whereas ammonia appeared in the presence of water in the same temperature range. Under special feed gas compositions further by-products, formaldehyde and hydrocarbons, were found over Cu/ZSM-5, whereas none of these compounds were observed over  $\gamma$ -alumina.

**Keywords:** NO<sub>x</sub>; Reduction; Alumina; By-products; Cu/ZSM-5

## 1. Introduction

Lean-burn gasoline and diesel fueled engines, which provide improved fuel economy as compared to conventional gasoline engines operating under stoichiometric air/fuel ratios, present new challenges for emission control, as they typically operate under net-oxidizing conditions, under which conventional three-way automotive catalysts show little ability to promote NO<sub>x</sub> reduction [1]. As a result, increased attention has been given

to the development of alternative catalyst systems that can reduce nitrogen oxides in the presence of oxygen.

For stationary combustion sources the selective catalytic reduction by NH<sub>3</sub> is still the most efficient technique for the removal of NO<sub>x</sub> in the presence of oxygen. However, the use of NH<sub>3</sub> as a reducing agent is not suitable for application in mobile combustion sources, such as lean burn engines. The more preferable use of hydrocarbons as reducing agents was reported for the catalytic reduction of NO<sub>x</sub> of HNO<sub>3</sub> plant tail gases [2,3], but the reaction was shown to be non-selective by

\* Corresponding author.

simultaneously facilitating the reaction of oxygen and nitrogen oxides with hydrocarbons. Recently, different types of zeolites with and without ion exchanged cations [4–21] as well as various metal oxides with and without transition metal additives [19–30] have been shown to selectively reduce  $\text{NO}_x$  with hydrocarbons in the presence of oxygen. However, high space velocity performance, selectivity behavior and durability of these catalysts in the presence of steam and sulphur oxides have to be improved to make application feasible.

Although many studies report the major nitrogen-containing product from  $\text{NO}_x$  reduction by hydrocarbons as being  $\text{N}_2$ , other species such as  $\text{NH}_3$  [29,33,34],  $\text{HCN}$  [15,29,31–34],  $\text{HNCO}$  [33],  $\text{N}_2\text{O}$  [15,28,29,32–34] and aliphatic cyanide species [16] have been observed in the gas phase. In addition, several studies have been reported, in which the course of the reaction has been followed by infrared spectroscopy. These investigations have been concerned mainly with the formation and removal of surface isocyanate species [17,18,25,26,30,35,36]. Unland [35,36] reported the formation of surface isocyanate species during the reaction of  $\text{NO}$  with  $\text{CO}$  on supported noble metal catalysts and hydrolysis of the surface isocyanate species was suggested to provide a pathway to  $\text{NH}_3$ . Harrison and Thornton [37] studied the mechanism of formation of surface isocyanate species from  $\text{NO}$  and  $\text{CO}$  over  $\text{CuO-SnO}_2$  and found, by the use of isotopic  $^{18}\text{O}$  substitution, that the  $\text{O}$  atom in this species originated from  $\text{NO}$ . Ukisu et al. [25,26] recently observed IR bands ascribable to adsorbed nitrogen containing species such as isocyanates and cyanides on  $\text{Cu/Al}_2\text{O}_3$  and  $\text{CuCs/Al}_2\text{O}_3$  catalysts during  $\text{NO}_x$  reduction by hydrocarbons. Adsorbed water or hydroxyl groups on the catalyst surface suppressed the formation of the isocyanate species.

Here we survey the formation of by-products such as hydrogen cyanide, cyanic acid, ammonia and nitrous oxide in the selective catalytic reduction of  $\text{NO}_x$  by either ethene or propene in the presence of excess oxygen over  $\gamma$ -alumina and

$\text{Cu/ZSM-5}$ . The effects of the nitrogen oxide ( $\text{NO}$  or  $\text{NO}_2$ ), of the hydrocarbon employed as a reducing agent ( $\text{C}_2\text{H}_4$  or  $\text{C}_3\text{H}_6$ ), and of water on the formation of the by-products and on the overall catalytic performance were examined. For this aim a specific experimental setup with a FT-IR spectrometer equipped with a gas cell for gas analysis was chosen, which allows the detection of any IR-active component in the gas phase.

## 2. Experimental

### 2.1. Catalyst preparation

Catalytic experiments were performed using  $\gamma$ -alumina and ion-exchanged  $\text{Cu/ZSM-5}$ . Aluminium oxide (Alumina C, Degussa) was agglomerated with deionized water, dried at 393 K, calcined in air at 873 K and crushed to a sieve fraction of 120–250  $\mu\text{m}$ . The BET surface area amounted to 109  $\text{m}^2 \text{g}^{-1}$  and XRD analysis indicated pure  $\gamma\text{-Al}_2\text{O}_3$ . The  $\text{Cu/ZSM-5}$  catalyst was prepared from  $\text{Na/ZSM-5}$  ( $\text{SiO}_2/\text{Al}_2\text{O}_3 = 44$ , Chemie Uetikon) by a standard ion-exchange method [15]. The copper loading of the catalyst, as determined by means of atomic absorption spectroscopy, was 2.6 wt.-%. BET surface areas determined by nitrogen adsorption measurements of both, the precursor  $\text{Na/ZSM-5}$  and the ion-exchanged catalyst, showed that the preparation procedure did not lead to a significant change of the surface area, which amounted to 373  $\text{m}^2 \text{g}^{-1}$  for both samples. The sieve fraction used for the catalytic measurements was 120–250  $\mu\text{m}$ .

### 2.2. Apparatus

#### 2.2.1. Gas mixing

A gas mixing manifold allows the composition of the desired feed gas concentrations, as specified in Table 1, by means of mass flow controllers (Brooks 5850E). Two streams of independently blended gases were mixed in a hot box (thermostated at 393 K), as shown in Fig. 1. The main stream contained the balance gas nitrogen, a

Table 1

Simulated exhaust compositions (feed gas mixtures) employed in catalytic studies; balance nitrogen

Feed No	1/(1w) <sup>a</sup>	2/(2w)	3/(3w)	4/(4w)
NO [ppm]	980/(940)	920/(940)	0	0
NO <sub>2</sub> [ppm]	0	0	970/(940)	980/(950)
C <sub>2</sub> H <sub>4</sub> [ppm]	0	1290/(1260)	0	1450/(1270)
C <sub>3</sub> H <sub>6</sub> [ppm]	910/(860)	0	910/(860)	0
O <sub>2</sub> [%]	2.0/(2.0)	2.0/(2.0)	1.9/(2.0)	1.9/(2.0)
H <sub>2</sub> O [%]	0/(10)	0/(10)	0/(10)	0/(10)

<sup>a</sup>Values in parenthesis correspond to feeds, containing 10% water, which are denoted with w.

hydrocarbon/nitrogen mixture and pure oxygen, when NO was chosen as NO<sub>x</sub> component. For gas mixtures containing NO<sub>2</sub> in place of NO, oxygen was fed into the 4.9% NO in nitrogen substream at room temperature by means of a three-way valve. The high partial pressure of oxygen and nitrogen monoxide together with a residence time of > 5 min facilitated the formation of NO<sub>2</sub>. No NO was detected for feeds 1 and 2 (Table 1), indicating that the conversion of NO to NO<sub>2</sub> was 100%. Other gases like CO, CO<sub>2</sub>, H<sub>2</sub> or SO<sub>2</sub> could be fed optionally into the substream. The purities of the component gases, as specified by the supplier (Pan Gas) were: O<sub>2</sub> (99.999%), N<sub>2</sub> (99.995%), 9.9% CO (99.9%) in nitrogen, 5.03% C<sub>2</sub>H<sub>4</sub> (99.5%) in nitrogen, 10% C<sub>3</sub>H<sub>6</sub> (99.5%) in nitrogen and 4.9% NO (99.0%) in nitrogen. All gases were used without further purification. Water was injected into the mainstream inside the hotbox via a separate tubing through a micro capillary (i.d. 0.18 mm) by means of a micro step pump.

After a mixing section of 8 m tube length, the gas flow was splitted into 4 equal flows using silica capillaries (length 500 mm, i.d. 0.32 mm). The resulting gas flow rates varied within  $\pm 5\%$ . One of the splitted flows was used to measure the feed concentration, whereas the other flows could be directed independently to the three U-tube quartz glass reactors (i.d. of 6 mm), which could be operated in series or parallel. The reactor effluent was either directed to the gas cell of the FT-IR spectrometer or to the purge.

## 2.2.2. Gas analysis

The Fourier Transform IR (FT-IR) spectrometer (Bruker IFS 66) used for gas analysis at the reactor inlet and outlet, respectively, was equipped with a heatable gas cell (100 ml volume; Infrared Analysis Inc.) and a MCT detector. To avoid condensation in the system, the gas cell and all tubings were heated at 393 K.

For calibration, absorbance FT-IR spectra (resolution 0.5 cm<sup>-1</sup>, 50 scans per spectrum) of specially prepared calibration gas mixtures with known concentrations were recorded for each component. Besides the gas mixtures, specified above, 2010 ppm N<sub>2</sub>O in argon (99.998%), 503.4 ppm NH<sub>3</sub> in argon (99.998%) and 197 ppm HCN in nitrogen have been used. Nitrogen was used for the background spectra. The calibration for CO<sub>2</sub> and H<sub>2</sub>O was done by oxidizing corresponding concentrations of ethene or propene at 866 K over

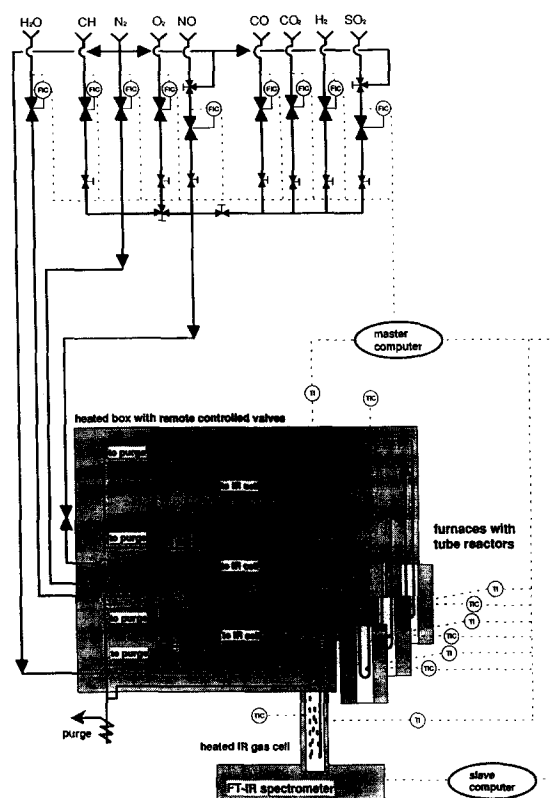


Fig. 1. Flow sheet of apparatus used for experimental measurements: Dotted lines correspond to electrical connections, straight lines correspond to gas tubings (except heated gas cell) and the grey zone corresponds to heated areas.

Table 2

Calibrated components with the number of calibration spectra, the integrated spectral range, the integration method and the calibrated range

component	number of spectra <sup>a</sup>	integrated spectral range [cm <sup>-1</sup> ]	integration method (cubic)	calibrated range [ppm]
Nitrogen monoxide	34	1872.14–1877.20	area	24–1752
Nitrogen dioxide	33 (24)	1612.00–1613.75	area	24–1947
Nitrous oxide	12	2213.9–2214.0	peak height	5–198
Ammonia	12	1082.7–1087.9	area	5–100
Hydrogen cyanide	9	712.3–712.7	peak height	5–101
Propene	35	2947–2957	area	24–1947
Ethene	35	2984–2992	area	24–2920
Carbon monoxide	39 (36)	2118–2133	area	24–2434
Carbon dioxide	34 (40)	2294.8–2296.7	area	73–5840
Water	34 (40)	1987–1994	area	73–5840

<sup>a</sup>Values in parenthesis correspond to a second calibration series.

1 wt.-% Pd/Al<sub>2</sub>O<sub>3</sub>. Nitrogen dioxide was calibrated by premixing 4.9% nitric oxide in nitrogen with oxygen. In these calibration spectra, no NO was found, indicating that the conversion to NO<sub>2</sub> was 100%.

Concentrations of each component were obtained by integration of specific absorption frequencies. In Table 2 the number of calibration spectra, the integration and calibration ranges for the components and the integration method are listed. An appropriate software package (OPUS vs. 2.0, Bruker) was used to calculate the concentrations of the feed and effluent gases. The accuracy in the concentration measurements by FT-IR was  $\pm 5\%$  for all components, as evidenced by measurements with calibration gas mixtures.

The concentration of nitrogen formed by reduction of NO<sub>x</sub> was calculated by using a mass balance over all nitrogen containing species (NO, NO<sub>2</sub>, N<sub>2</sub>O, NH<sub>3</sub> and HCN). The selectivity to N<sub>2</sub> is calculated according to:  $S_N = 1 - [\sum N - \text{products}] / [(NO_x)_{in} - (NO_x)_{out}]$ , where NO<sub>x</sub> is the sum of NO and NO<sub>2</sub>, and  $\sum N$ -products represents all nitrogen containing products, except N<sub>2</sub>.

### 2.2.3. Spectra recording

Nitrogen was used for background measurements. Spectra were recorded after purging the gas cell for 200 s with nitrogen (3.5 l (STP)/min). Before measuring the gas mixtures at the inlet and the outlet of the reactors, the gas cell was

again purged for 200 s and two spectra were taken within 400 s. For any temperature step, the reactant gas at the inlet was analyzed to monitor the inlet concentrations with time. With three catalysts mounted in the system, a total of 80 min per temperature step was used to analyze the catalysts and the inlet concentrations. Having 10% water in the feed stream (wet feeds) another 30 min was waited, to allow the catalysts to reach steady-state.

### 2.2.4. System control

A master computer is used to control remote settings and a software package written in our group allows timed programming of a series of setpoints. The FT-IR station was set into a slave mode to the master computer by means of a TTL signal.

### 2.3. Catalytic measurements

Before the catalytic experiments, the catalysts were pretreated at 873 K for 2 h in 5% oxygen in nitrogen, followed by cooling the catalyst to 473 K in nitrogen. Subsequently, reaction gas, as listed in Table 1, was passed over the catalyst beds with a flow rate of 150 ml(STP)/min for 2 h. The temperature dependence of the catalytic behavior was measured by raising the temperature in steps of 50 K from 473 to 873 K.

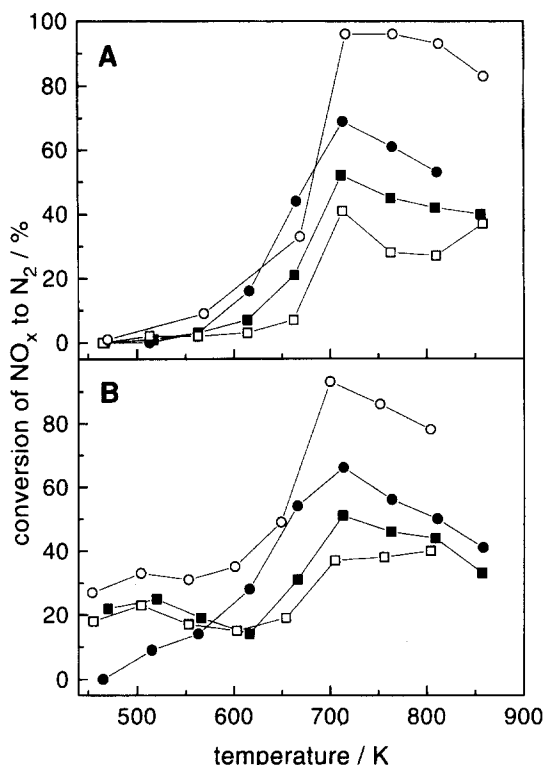


Fig. 2. Temperature dependence of conversions of  $\text{NO}_x$  to nitrogen with ( $\square, \blacksquare$ ) propene and with ( $\circ, \bullet$ ) ethene over Cu/ZSM-5. (A) Conversion of NO to nitrogen and (B) conversion of  $\text{NO}_2$  to nitrogen. Open symbols correspond to feeds without additional water, filled symbols to feeds containing 10% water (Table 1).  $W/F = 0.1 \text{ g s ml}^{-1}$ .

### 3. Results and discussion

#### 3.1. Catalytic activity

Fig. 2 summarizes the activity measurements for Cu/ZSM-5 for the feeds specified in Table 1. Comparing Fig. 2A with Fig. 2B shows that the activity for the selective catalytic reduction of  $\text{NO}_x$  is not sensitive on the type of nitrogen oxide, but on the type of hydrocarbon used. With ethene nearly complete conversion is reached with both NO and  $\text{NO}_2$ , whereas with propene the maximal  $\text{NO}_x$  conversion reaches only 50% at 712 K. Matsumoto et al. [38] also found that over Cu/ZSM-5, the type of hydrocarbon plays a dominant role in the course of the reaction to nitrogen.

Water reduces the influence of the type of hydrocarbon as can be seen by comparing either feed 1w with feed 2w and feed 3w with 4w, respec-

tively. When wet feeds are used, the reduction activity of the propene containing feed increases (Fig. 2B) while with ethene a marked decrease is observed.

In contrast to Cu/ZSM-5, with  $\gamma$ -alumina as a catalyst the type of nitrogen oxide strongly determines the reduction activity, whereas the hydrocarbon used is of minor importance (Fig. 3A and Fig. 3B). Nitric oxide as the major type of  $\text{NO}_x$  in the exhaust is not effectively reduced, while with  $\text{NO}_2$  conversion of up to 93% is achieved at 666 K for both alkenes. At temperatures above 700 K the reduction activity with ethene remains constant, while with propene the formation of nitrogen decreases. Water affects the reduction activities of both hydrocarbons in a similar way, leading to a decrease of the formation of nitrogen, but with  $\text{NO}_2$  still being more easily reduced than NO.

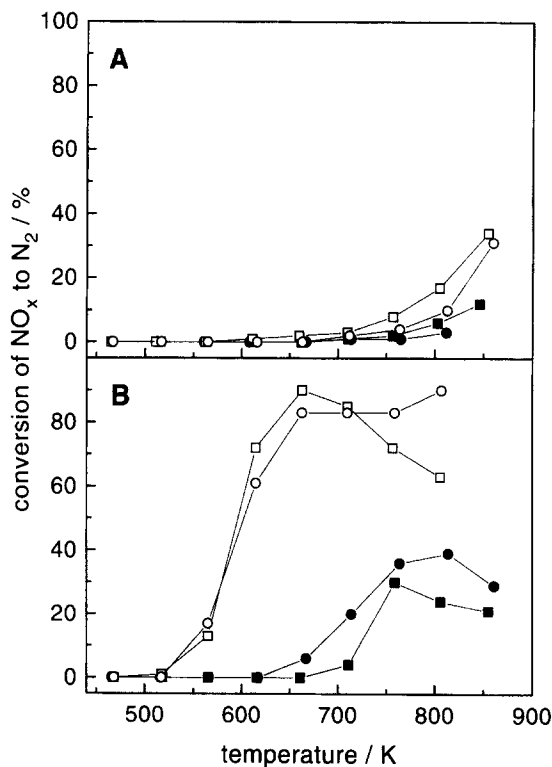


Fig. 3. Temperature dependence of conversions of  $\text{NO}_x$  to nitrogen with ( $\square, \blacksquare$ ) propene and with ( $\circ, \bullet$ ) ethene over  $\gamma$ -alumina. (A) Conversion of NO to nitrogen and (B) conversion of  $\text{NO}_2$  to nitrogen. Open symbols correspond to feeds without additional water, filled symbols to feeds containing 10% water (Table 1).  $W/F = 0.1 \text{ g s ml}^{-1}$ .

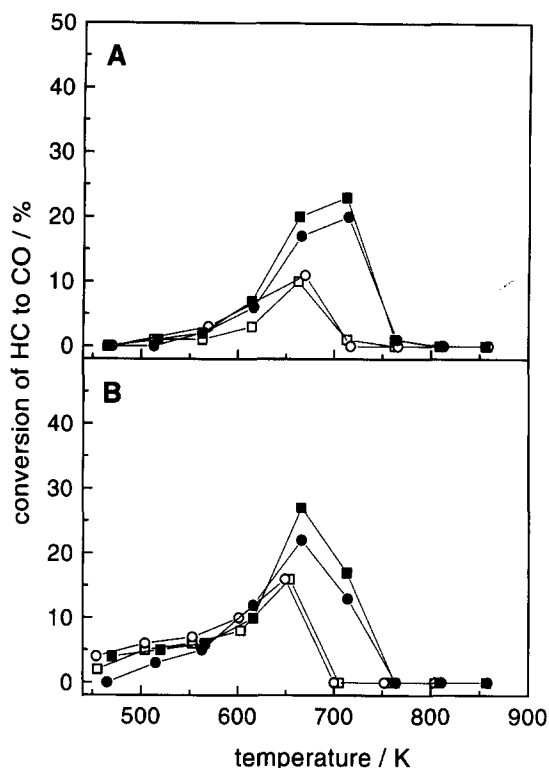


Fig. 4. Temperature dependence of conversions of the hydrocarbons to carbon monoxide with ( $\square, \blacksquare$ ) propene and with ( $\circ, \bullet$ ) ethene over Cu/ZSM-5 for (A) feeds containing NO and (B) feeds containing NO<sub>2</sub>. Open symbols correspond to feeds without additional water, filled symbols to feeds containing 10% water (Table 1).  $W/F = 0.1 \text{ g s ml}^{-1}$ .

### 3.2. Formation of by-products

#### 3.2.1. Carbon monoxide

In Fig. 4A and Fig. 4B the formation of carbon monoxide as a by-product of the catalytic after treatment is depicted for the Cu/ZSM-5 catalyst. Both hydrocarbons show a similar tendency for CO formation, which is not significantly affected by the type of NO<sub>x</sub>. This supports the findings of Matsumoto et al. [38] who stated, that the rate of decrease of the hydrocarbon is independent of the NO<sub>x</sub> component and that the conversion of NO<sub>x</sub> is subordinate to the reaction of the hydrocarbon with oxygen. In the presence of water the formation of CO increased and its maximum shifted towards higher temperature (from 15% at 666 K to 27% at 719 K for Feed 3/3w).

With alumina, the formation of carbon monoxide is influenced by the type of NO<sub>x</sub>, whereas

the hydrocarbon shows a less pronounced influence (Fig. 5A and Fig. 5B). With NO, a similar tendency is observed for ethene and propene with the latter producing slightly more CO. Water has an opposite effect by enhancing CO formation with propene and suppressing it with ethene. Starting from NO<sub>2</sub>, two temperature regimes of CO production can be distinguished with the low temperature regime being superimposed on the CO formation observed with NO. As compared to NO, significantly more carbon monoxide is produced for corresponding temperatures and the onset of CO formation occurs already at 570 K, as compared to 710 K with NO. Water again suppresses CO formation with ethene, whereas with propene more CO is produced at higher temperatures.

#### 3.2.2. Hydrogen cyanide

Concerning the formation of hydrogen cyanide over Cu/ZSM-5, with ethene as a reductant a similar behavior was found for both types of NO<sub>x</sub> (Fig. 6A and Fig. 6B). Maximum HCN concentration ranges from 18 to 25 ppm around 610 K, irrespective of whether water is present or not. With propene the type of NO<sub>x</sub> and the presence of water largely influence the formation of HCN. Markedly higher concentrations of HCN are found with NO<sub>2</sub> yielding 30 ppm at 510 K while with NO only 4 ppm were formed at 562 K. Addition of water further increased the hydrogen cyanide formation. A maximum concentration of 38 ppm at 520 K, followed by a second maximum of 21 ppm at 660 K is observed with nitrogen dioxide (feed 3w), whereas with nitric oxide (feed 1w) 10 ppm HCN were measured at 660 K.

Over alumina the formation of hydrogen cyanide is greatly influenced by the type of hydrocarbon, the type of nitrogen oxide and the presence of water (Fig. 7A and Fig. 7B). Generally, higher concentrations of hydrogen cyanide were found using propene as a reductant and HCN formation occurred at significantly lower temperature with feeds containing NO<sub>2</sub>. Maximum HCN concentrations of 68 ppm at 565 K with feed 3 and of 18 ppm at 850 K with feed 1 were measured for propene, whereas HCN production remained

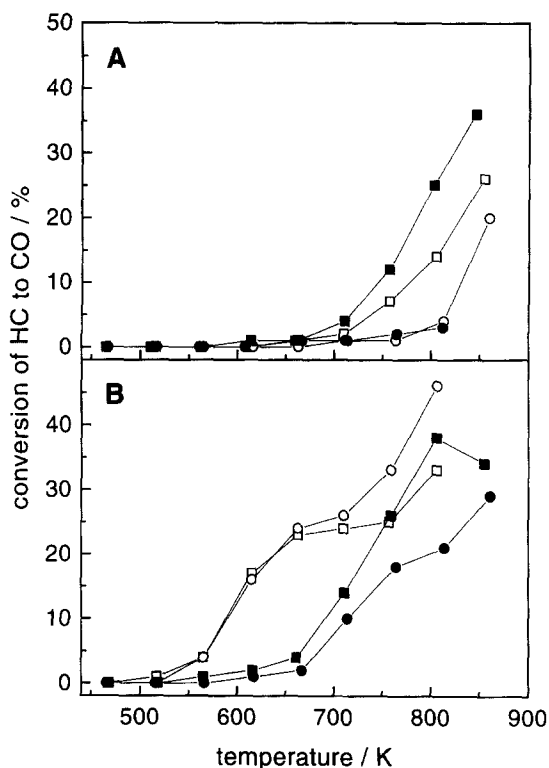


Fig. 5. Temperature dependence of the conversions of the hydrocarbons to carbon monoxide with ( $\square, \blacksquare$ ) propene and with ( $\circ, \bullet$ ) ethene over  $\gamma$ -alumina for (A) feeds containing NO and (B) feeds containing  $\text{NO}_2$ . Open symbols correspond to feeds without additional water, filled symbols to feeds containing 10% water (Table 1).  $W/F = 0.1 \text{ g s ml}^{-1}$ .

below 10 ppm for ethene containing feeds. Addition of water generally suppressed HCN formation, resulting in 10 ppm for feed 3w, while no HCN could be observed for the other feeds.

### 3.2.3. Cyanic acid and ammonia

Besides CO and HCN, substantial amounts of cyanic acid were produced over Cu/ZSM-5 with dry feeds, reaching a maximum of ca. 15 ppm at 666 K for feed 3, while ammonia formation was negligible. With 10% water in the feed (feed 3w), HNCO disappeared and ammonia was found in the same temperature range, with concentrations up to 8 ppm at 666 K. In a study of the reduction of NO with CO and  $\text{H}_2$  on precious-metal catalysts, Voorhoeve and Trimble [39] also observed ammonia in the gas phase. A low temperature peak was attributed to the formation of  $\text{NH}_3$  via hydrolysis of an isocyanate intermediate.

Although bands due to HNCO were observed with ethene under dry conditions (feed 2 and 4), no ammonia was detected under wet conditions which may be explained by the higher detection limit for ammonia (8 ppm) when ethene is used [33]. With alumina, no HNCO could be detected and ammonia formation was hardly observable independently of the feed composition.

### 3.2.4. Other by-products

Nitrous oxide concentrations up to 10 ppm were found with Cu/ZSM-5 irrespective of the feed composition, but with dry feeds resulting in slightly higher  $\text{N}_2\text{O}$  concentrations. With alumina  $\text{N}_2\text{O}$  formation remained low, except for feeds containing  $\text{NO}_2$ , where 10 ppm  $\text{N}_2\text{O}$  were observed. While no further by-products could be observed over  $\gamma$ -alumina, formaldehyde, ethene and methane were identified in different temperature regimes over Cu/ZSM-5 with feed 1 and 3.

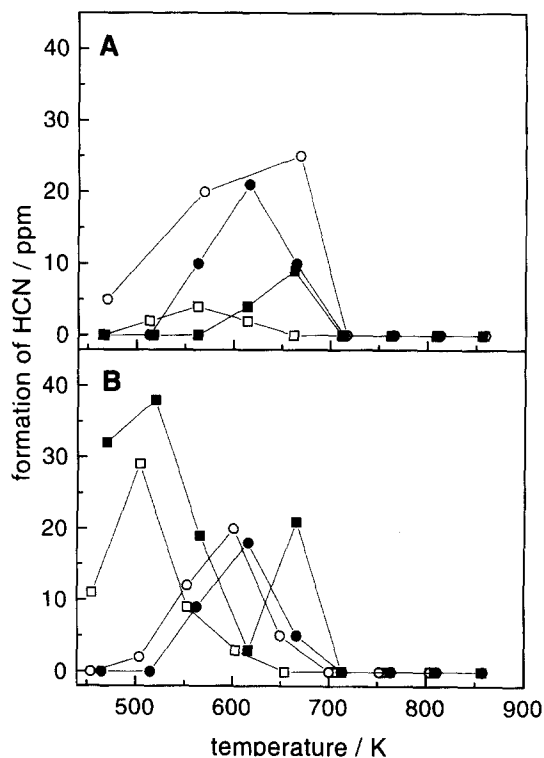


Fig. 6. Temperature dependence of the formation of hydrogen cyanide with ( $\square, \blacksquare$ ) propene and with ( $\circ, \bullet$ ) ethene over Cu/ZSM-5 for (A) feeds containing NO and (B) feeds containing  $\text{NO}_2$ . Open symbols correspond to feeds without additional water, filled symbols to feeds containing 10% water (Table 1).  $W/F = 0.1 \text{ g s ml}^{-1}$ .

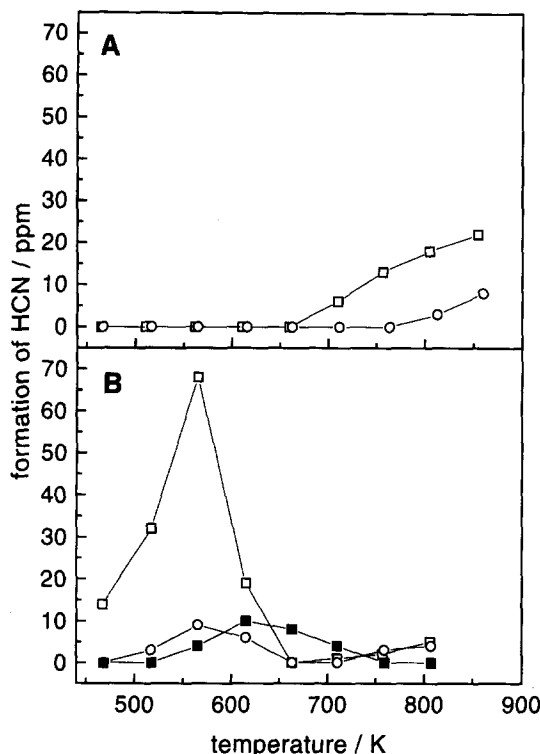


Fig. 7. Temperature dependence of the formation of hydrogen cyanide with ( $\square, \blacksquare$ ) propene and with ( $\circ, \bullet$ ) ethene over  $\gamma$ -alumina for (A) feeds containing NO and (B) feeds containing  $\text{NO}_2$ . Open symbols correspond to feeds without additional water, filled symbols to feeds containing 10% water (Table 1).  $W/F = 0.1 \text{ g s ml}^{-1}$ .

#### 4. Conclusions

The catalytic performance as well as the formation of undesired by-products in the selective catalytic reduction of nitrogen oxides by alkenes in excess oxygen are strongly governed by the catalyst, the hydrocarbon used as a reductant, the nitrogen oxide (NO or  $\text{NO}_2$ ) and the presence of water. Substantial quantities of undesirable by-products such as CO, HCN, HNCO,  $\text{NH}_3$ ,  $\text{N}_2\text{O}$  and  $\text{CH}_2\text{O}$  are formed under certain experimental conditions. With alumina,  $\text{NO}_2$  is reduced more efficiently than NO with both reductants but with ethene showing a lower tendency to form undesired by-products. Water addition strongly suppresses catalytic activity and formation of by-products. This contrasts the findings with Cu/ZSM-5, where HCN formation is not altered by the presence of water and where ammonia appears in place of HNCO upon adding water.

#### Acknowledgements

We thank S. Tagliaferri for his important contribution on the program for the system control.

#### References

- [1] K.C. Taylor, *Catal. Rev.-Sci. Eng.*, 35 (1993) 457.
- [2] H.C. Anderson, W.J. Green and D.R. Steele, *Ind. Eng. Chem.*, 53 (1961) 199.
- [3] R.A. Searles, *Platinum Met. Rev.*, 17 (1973) 57.
- [4] M. Iwamoto, H. Yahiro, S. Shundo, Y. Yu-u and N. Mizuno, *Shokubai (Catal.)*, 32 (1990) 430.
- [5] W. Held, A. König, T. Richter and L. Puppe, SAE Technical Paper Series (Society of Automotive Engineers paper 900496), 810 (1990) 13.
- [6] S. Sato, Y. Yu-u, H. Yahiro, N. Mizuno and M. Iwamoto, *Appl. Catal.*, 70 (1991) L1.
- [7] C.J. Bennet, P.S. Bennett, S.E. Golunski, J.W. Hayes and A.P. Walker, *Appl. Catal. A: General*, 86 (1992) L1.
- [8] C.N. Montreuil and M. Shelef, *Appl. Catal. B: Environmental*, 1 (1992) L1.
- [9] Y. Li and J. Armor, *Appl. Catal. B: Environmental*, 1 (1992) L31.
- [10] Y. Li, P.J. Battavio and J.N. Armor, *J. Catal.*, 142 (1993) 561.
- [11] B.K. Cho, *J. Catal.*, 142 (1993) 418.
- [12] K.C.C. Kharas, *Appl. Catal. B: Environmental*, 2 (1993) 207.
- [13] R. Burch and P.J. Millington, *Appl. Catal. B: Environmental*, 2 (1993) 101.
- [14] J.O. Petunchi, G. Sill and W.K. Hall, *Appl. Catal. B: Environmental*, 2 (1993) 303.
- [15] F. Radtke, R.A. Koepfel and A. Baiker, *Appl. Catal. A: General*, 107 (1994) L125.
- [16] N. Hayes, W. Grünert, G. Hutchings, R. Joyner and E.J. Shpiro, *Chem. Soc., Chem. Commun.*, (1994) 531.
- [17] V.A. Bell, J.S. Feeley, M. Deeba and R.J. Farrauto, *Catal. Lett.*, 29 (1994) 15.
- [18] H. Yasuda, T. Miyamoto and M. Misono, *ACS Div. Petr. Chem.*, 39 (1994) 99.
- [19] M. Sasaki, H. Hamada, Y. Kintaichi and T. Ito, *Catal. Lett.*, 15 (1992) 297.
- [20] H. Hamada, Y. Kintaichi, T. Yoshinari, M. Tabata, M. Sasaki and T. Ito, *Catal. Today*, 17 (1993) 111.
- [21] M. Iwamoto, N. Mizuno and H. Yahiro, *New Frontiers in catalysis, Proc. of the 10th Int. Congr. on Catal., Budapest, 19–24 July, Studies in Surface Science and Catalysis, Vol. 75, Elsevier, Amsterdam, 1992, p. 213.*
- [22] H. Hamada, Y. Kintaichi, M. Sasaki, T. Ito and M. Tabata, *Appl. Catal.*, 75 (1991) L1.
- [23] Y. Torikai, H. Yahiro, N. Mizuno and M. Iwamoto, *Catal. Lett.*, 9 (1991) 91.
- [24] Y. Kintaichi, H. Hamada, M. Tabata, M. Sasaki and T. Ito, *Catal. Lett.*, 6 (1991) 239.
- [25] Y. Ukisu, S. Sato, G. Muramatsu and K. Yoshida, *Catal. Lett.*, 11 (1991) 177.



- [26] Y. Ukisu, S. Sato, A. Abe and K. Yoshida, *Appl. Catal. B: Environmental*, 2 (1993) 147.
- [27] S. Subramanian, R.J. Kudla, W. Chun and S. Chattha, *Ind. Eng. Chem. Res.*, 32 (1993) 1805.
- [28] A. Obuchi, A. Ohi, M. Nakamura, A. Ogata, K. Mizuno and H. Obuchi, *Appl. Catal. B: Environmental*, 2 (1993) 71.
- [29] F. Radtke, R.A. Koeppel and A. Baiker, *Catal. Lett.*, 28 (1994) 131.
- [30] G.R. Bamwenda, A. Obuchi, A. Ogata and K. Mizuno, *Chem. Lett.*, (1994) 2109.
- [31] C. Yokoyama and M. Misono, *J. Catal.*, 150 (1994) 9.
- [32] H. Yasuda, T. Miyamoto and M. Misono, *Am. Chem. Soc., Div. Petr. Chem.*, 39 (1994) 99.
- [33] F. Radtke, R.A. Koeppel and A. Baiker, *J. Chem. Soc., Chem. Commun.*, (1995) 427.
- [34] F. Radtke, R.A. Koeppel and A. Baiker, *Environ. Sci. Technol.*, in press.
- [35] M.L. Unland, *J. Catal.*, 31 (1973) 459.
- [36] M.L. Unland, *J. Phys. Chem.*, 77 (1973) 1952.
- [37] P.G. Harrison and E.W. Thornton, *J. Chem. Soc., Faraday Trans. 1*, 74 (1978) 2604.
- [38] S. Matsumoto, K. Yokota, H. Doi, M. Kimura, K. Sekizawa and S. Kasahara, *Catal. Today*, 22 (1994) 127.
- [39] R.J.H. Voorhoeve and L.E. Trimble, *J. Catal.*, 38 (1975) 34.